

METHOD OF CHARACTERISTICS SOLUTIONS FOR NON-EQUILIBRIUM TRANSIENT FLOW-BOILING

R. L. FERCH

Atomic Energy of Canada Ltd., Whiteshell Nuclear Research Establishment, Pinawa, Manitoba ROE 1LO,
 Canada

(Received 2 February 1978; in revised form 28 April 1979)

Abstract—A method of characteristics algorithm for the equal velocity, unequal temperature model of one-dimensional two-phase flow has been implemented. This algorithm uses a mesh of characteristics $dz/dt = u \pm a$, and has greatly reduced numerical diffusion effects when compared with finite difference methods, making it useful for benchmark solutions and model testing. Results are presented from its applications to two standard problems.

INTRODUCTION

The analysis of transient two-phase flow phenomena is of much interest in the design and licensing of nuclear power reactors. The simplest model, in which the vapour and liquid phases have equal velocities and temperatures (the EVET model), is widely used (Martini *et al.* 1976, Mathers 1976, Turner & Trimble 1976). However, the importance of thermal non-equilibrium and unequal velocity effects has stimulated interest in more sophisticated (or perhaps more physically representative) models (Banerjee *et al.* 1978, Boure *et al.* 1973, Brittan & Fayers 1976, Solbrig *et al.* 1976). The model considered here is of intermediate sophistication; the phases have the same velocity, but are allowed to have unequal temperatures (the EVUT model) (Hancox *et al.* 1975).

Rapid finite difference solution procedures are being developed to study the EVUT model. These methods are subject to numerical diffusion and other numerical errors. To determine the magnitude of these errors, a benchmark solution procedure is needed which provides close approximations to the true mathematical solutions of the EVUT equations. Also, to determine the interphase transfer coefficients we use specially designed experiments along with benchmark solutions to the EVUT equations. Because these equations are of the hyperbolic type, we have developed a benchmark solution based on a method of characteristics wave-tracing procedure. The solution scheme is similar to one previously used for the same purposes with the EVET model (Hancox & Banerjee 1977, Hancox *et al.* 1975). This paper describes the EVUT model, the wave-tracing algorithm used in the benchmark program, and some results obtained using this program on standard problems.

We begin by writing the conservation-law equations for one-dimensional two-phase flow, neglecting viscosity and axial heat flux terms (Hancox *et al.* 1975, Boure 1973):

$$A \frac{\partial}{\partial t} \alpha_k \rho_k + \frac{\partial}{\partial z} A \alpha_k \rho_k u_k = m_{ik} \quad [1]$$

$$A \frac{\partial}{\partial t} \alpha_k \rho_k u_k + \frac{\partial}{\partial z} A \alpha_k \rho_k u_k^2 + A \alpha_k \frac{\partial}{\partial z} p_k = m_{ik} u_k - \tau_{ik} - \tau_{wk} - A \alpha_k \rho_k g \frac{dz}{dz} \quad [2]$$

$$A \frac{\partial}{\partial t} \alpha_k \rho_k \left(h_k + \frac{1}{2} u_k^2 \right) + \frac{\partial}{\partial z} A \alpha_k \rho_k u_k \left(h_k + \frac{1}{2} u_k^2 \right) - A \alpha_k \frac{\partial}{\partial t} p_k \\ = q_{ik} + q_{wk} + \tau_{ik} u_k + m_{ik} \left(h_k + \frac{1}{2} u_k^2 \right) - A \alpha_k \rho_k u_k g \frac{dz}{dz}. \quad [3]$$

In these equations, the subscript $k (=f \text{ or } g)$ denotes the phase (liquid or vapor). The flow

quantities α_k , ρ_k , u_k , p_k and h_k are the volume fraction, density, axial velocity, pressure, and specific enthalpy of phase k respectively. The source terms m_{ik} , τ_{ik} , q_{ik} and q_{wk} are the mass transfer rate at the interface, interfacial friction, interfacial heat transfer and wall heat transfer into phase k respectively. A is the cross-sectional area of the duct, Z the elevation, g the gravitational acceleration, and t and z are the time and space independent variables.

The phase volume fractions satisfy $\alpha_g + \alpha_f = 1$. We have assumed gravity to be the only external body force acting. In order that mass, momentum and energy be conserved at the interface between phases, the following relations also must hold:

$$m_{ig} + m_{if} = 0 \quad [4]$$

$$m_{ig}u_g - \tau_{ig} + m_{if}u_f - \tau_{if} = 0 \quad [5]$$

$$q_{ig} + \tau_{ig}u_g + m_{ig}\left(h_g + \frac{1}{2}u_g^2\right) + q_{if} + \tau_{if}u_f + m_{if}\left(h_f + \frac{1}{2}u_f^2\right) = 0. \quad [6]$$

In the EVUT model, we assume $p_f = p_g = p$, $u_f = u_g = u$ and $\tau_{if} = \tau_{ig} = 0$. Keeping [1] and [3] from both liquid and vapour, and summing the momentum equations [2] for the two phases, we obtain, after some manipulation,

$$\frac{\partial}{\partial t} \alpha_k \rho_k + \frac{\partial}{\partial z} \alpha_k \rho_k u = \frac{m_{ik}}{A} - \alpha_k \rho_k u \frac{1}{A} \frac{dA}{dz} \quad [7]$$

$$\rho \frac{\partial u}{\partial t} + \rho u \frac{\partial u}{\partial z} + \frac{\partial p}{\partial z} = -\frac{\tau_{wf} + \tau_{wg}}{A} - \rho g \frac{dZ}{dz} \quad [8]$$

$$\alpha_k \rho_k \frac{\partial}{\partial t} h_k + \alpha_k \rho_k u \frac{\partial}{\partial z} h_k - \alpha_k \frac{\partial p}{\partial t} - \alpha_k u \frac{\partial p}{\partial z} = \frac{q_{ik} + q_{wk} + \tau_{wk} u}{A} \quad [9]$$

where the mixture density $\rho = \alpha_g \rho_g + \alpha_f \rho_f$.

In order to close this set, constitutive relations are needed. The first of these are the equations of state, in the form $\rho_k = \rho_k(p, h_k)$. The duct cross section, $A(z)$, and elevation, $Z(z)$, are specified for each problem. Before giving our formulae for q_{ik} , q_{wk} , τ_{wk} and m_{ik} , we note the following conditions: In order that [7]–[9] be non-singular, and reduce to the single-phase equations when $\alpha_k = 0$ or 1, we require $\lim_{\alpha_k \rightarrow 0} (q_{ik}/\alpha_k)$, (q_{wk}/α_k) , (τ_{wk}/α_k) and (m_{ik}/α_k) to be finite,

and $\lim_{\alpha_k \rightarrow 1} q_{ik}/(1-\alpha_k)$ and $m_{ik}/(1-\alpha_k)$ to be finite. We will assume in what follows that the

constitutive terms q_{ik} , q_{wk} , τ_{wk} and m_{ik} depend only on the local instantaneous flow variables. That is, derivatives of the flow variables will not be allowed in these terms.

To specify q_{ik} , we let $q_{ik} = \lambda_{ik}(T_s - T_k)$, where λ_{ik} is the interface thermal conductivity, then write $\lambda_{ik} = K_{ik} A_i \rho_k c_{pk}$, where A_i is the interfacial area per unit length, and K_{ik} has the dimensions of m/sec. Replace $c_{pk}(T_s - T_k)$ by $h_{ks} - h_k$, and let $K_{ik} A_i = \alpha_f \alpha_g A / t_{ik}$. The parameter t_{ik}^{-1} can be considered to be a rate constant for the interfacial heat transfer process, and models of any desired degree of complexity can be constructed by appropriate calculations of t_{ik} . In our case, we have assumed $t_{ik} = \text{constant}$, which is the result achieved by assuming $A_i \propto \alpha_f \alpha_g A$, constant c_{pk} , and constant K_{ik} ; our form for q_{ik} is $q_{ik} = \alpha_f \alpha_g A \rho_k (h_{ks} - h_k) / t_{ik}$. This form was chosen not because of any expected physical validity, although it should be adequate as a rough approximation, but because of its simplicity. This is in keeping with the intent of the program, which is used as a mathematical benchmark. From [4] and [6], $m_{ig} = -m_{if} = -(q_{if} + q_{ig}) / (h_g - h_f)$. For q_{wk} we use $q_{wk} = \alpha_k q_w$ where q_w is given as a function of z ; this simplified model neglects the heat content of the wall. For the frictional terms, we use $\tau_{wk} = \alpha_k \rho_k A F$, with $F = ((4f/D_e) + (K/l))(u|u|/2)$, and the equivalent diameter D_e and distributed loss coefficient K/l are given functions of z . The friction factor f , when $\alpha_f = 1$, is $0.046 R_f^{-0.2}$,

for $R_f > 1462.27$, and $64/R_f$ for $R_f < 1462.27$; when $\alpha_g = 1$, R_f is replaced by R_g . For $0 < \alpha_f < 1$, $f = \tau^* f$ ($\alpha_f = 1$), where τ^* is the two-phase multiplier (Hancox & Nicoll 1972):

$$\tau^* = 1 + \chi(\beta - 1)\{1 + 3.57 \exp(-0.00994\gamma)[1 - \exp\{-4.96(1 - \chi)\}]\} \quad [10]$$

where $\chi = \alpha_g \rho_g / \rho$ is the flow quality, and

$$\gamma = \frac{\rho|u|}{[g\rho_f(\rho_f - \rho_g)\eta_f]^{1/3}}$$

$$\beta = \frac{\rho_f}{\rho_g} \left(\frac{\eta_g}{\eta_f} \right)^{0.2}.$$

Here η_k is the dynamic viscosity, and $R_k = \rho_k|u|/\eta_k$ is the Reynolds number. The division point $R = 1462.27$ is chosen so that the formulation will be continuous.

After using the equations of state and the differentiation chain-rule for the first two terms of [7], and taking the appropriate linear combinations of [7], [8] and [9], we obtain the characteristic form:

$$\frac{\partial p}{\partial t} + (u + a) \frac{\partial p}{\partial z} + \rho a \left[\frac{\partial u}{\partial t} + (u + a) \frac{\partial u}{\partial z} \right] = \rho a^2 C_1 + a C_2 \quad [11]$$

$$\frac{\partial p}{\partial t} + (u - a) \frac{\partial p}{\partial z} - \rho a \left[\frac{\partial u}{\partial t} + (u - a) \frac{\partial u}{\partial z} \right] = \rho a^2 C_1 - a C_2 \quad [12]$$

$$\frac{\partial \alpha}{\partial t} + u \frac{\partial \alpha}{\partial z} + \alpha(1 - \alpha) \left(\frac{1}{\rho_g a_g^2} - \frac{1}{\rho_f a_f^2} \right) \left[\frac{\partial p}{\partial t} + u \frac{\partial p}{\partial z} \right] = C_3 \quad [13]$$

$$\frac{\partial h_g}{\partial t} + u \frac{\partial h_g}{\partial z} - \frac{1}{\rho_g} \left[\frac{\partial p}{\partial t} + u \frac{\partial p}{\partial z} \right] = C_4 \quad [14]$$

$$\frac{\partial h_f}{\partial t} + u \frac{\partial h_f}{\partial z} - \frac{1}{\rho_f} \left[\frac{\partial p}{\partial t} + u \frac{\partial p}{\partial z} \right] = C_5. \quad [15]$$

We define $\alpha = \alpha_g = 1 - \alpha_f$,

$$a^{-2} = \rho \left[\frac{\alpha}{\rho_g a_g^2} + \frac{1 - \alpha}{\rho_f a_f^2} \right],$$

and

$$a_k^{-2} = \frac{\partial \rho_k}{\partial p} + \frac{1}{\rho_k} \frac{\partial \rho_k}{\partial h_k}.$$

The C_i are given by

$$C_1 = \left(\frac{1}{\rho_g} - \frac{1}{\rho_f} \right) \frac{m_{ig}}{A} - u \frac{1}{A} \frac{dA}{dz} - \frac{\alpha}{\rho_g} \frac{\partial \rho_g}{\partial h_g} C_4 - \frac{(1 - \alpha)}{\rho_f} \frac{\partial \rho_f}{\partial h_f} C_5,$$

$$C_2 = -\frac{\tau_{wf} + \tau_{wg}}{A} - \rho g \frac{dZ}{dz},$$

$$C_3 = \frac{\rho}{\rho_f \rho_g} \frac{m_{ig}}{A} - \alpha(1 - \alpha) \left[\frac{1}{\rho_g} \frac{\partial \rho_g}{\partial h_g} C_4 - \frac{1}{\rho_f} \frac{\partial \rho_f}{\partial h_f} C_5 \right],$$

$$C_4 = \frac{q_{ig} + q_{wg} + \tau_{wg} u}{\alpha \rho_g A},$$

and

$$C_5 = \frac{q_{if} + q_{wf} + \tau_{wf} u}{(1 - \alpha) \rho_f A}.$$

After specifying the initial state of the system, $A(z)$, $Z(z)$, $q_w(z)$, $D_e(z)$, $K/l(z)$, the equations of state $\rho_k = \rho_k(p, h_k)$ along with $\partial\rho_k/\partial p$, $\partial\rho_k/\partial h_k$ and $\eta_k(p, h_k)$, and the boundary conditions, the mathematical specification of the problem is complete. The boundary conditions used are the following: At a closed boundary, $u = 0$. At an outflow boundary, p is specified, provided that $|u| < a$; if this condition is not satisfied, $|u| = a$ is specified instead, and p is increased until agreement is reached. At an inflow boundary, p , α , h_f and h_g are specified; if this leads to $|u| > a$, we specify $|u| = a$.

Note that the assumption of no derivatives in the constitutive terms is necessary in order to achieve this form. If derivatives of the flow variables were to appear in the constitutive terms, the structure of the equation set would be altered. The characteristic directions ($u + a$, $u - a$, u , u) would be changed, and in general would not be real. The method of characteristics described below requires: (a) that the system of equations be hyperbolic (real characteristics) and (b) that the characteristic equations be expressible analytically. Therefore, this method may not be applicable to models in which such derivative dependence is allowed.

WAVE-TRACING ALGORITHM

Equations [11]–[15] may be rewritten in the form of paired characteristic and compatibility relations, as

$$dz = (u + a) dt; dp + \rho a du = (\rho a^2 C_1 + a C_2) dt, \quad [16]$$

$$dz = (u - a) dt; dp - \rho a du = (\rho a^2 C_1 - a C_2) dt, \quad [17]$$

$$dz = u dt; d\alpha - \alpha(1 - \alpha) \left[\frac{1}{\rho_f a_f^2} - \frac{1}{\rho_g a_g^2} \right] dp = C_3 dt, \quad [18]$$

$$dz = u dt; dh_g - \frac{1}{\rho_g} dp = C_4 dt, \quad [19]$$

$$dz = u dt; dh_f - \frac{1}{\rho_f} dp = C_5 dt. \quad [20]$$

These equations approximated by simple first-order difference equations, in which all coefficients are evaluated by taking the averages of their values at the two points involved. The grid of points at which the solution is calculated is not the usual grid of points fixed in space and time; rather, it consists of the points at which a set of characteristic curves $dz/dt = u \pm a$ intersect. (These curves are the paths along which small-amplitude sound waves propagate; hence the term “wave-tracing”.) For simplicity, we will call these curves “waves”, and their intersection points “nodes”. A second set of points, called “particles”, are at the intersection points of the waves with a number of “streamlines” $dz/dt = u$. The number of streamlines used in the discretization is, in general, different from the number of waves defining the primary mesh. This secondary mesh of “particles” is used mainly for diagnostic purposes, to aid in studying the motion of the fluid itself. The algorithm used to calculate the independent and dependent variables at a node N_j is illustrated in figure 1; the notation used is $\Delta\psi_{mn} = \psi_m - \psi_n$, $[\psi]_{mn} = \frac{1}{2}(\psi_m + \psi_n)$. Since the coefficients in the difference equations depend on the solution at node N_j , an iterative technique is used to generate a self-consistent solution. The interpolated point O is discarded once the solution for node N_j is known. Once the solution at N_j has been calculated, the particles P_i lying between nodes N_{j-1} and N_{j+1} are advanced to their new positions (see figure 2). Again, an iterative method is used.

A number of variations on this scheme are also possible. In the illustrated scheme, P_i and N'_j were chosen because they are the nearest points to O on $N_{j-1}N'_j$; they may be either nodes or particles. Instead, point O may be interpolated between P_i and P_{i+1} , or between N_{j-1} and N_{j+1} . In either of these cases, the interpolation is (usually) not along a characteristic direction, as it is in the first case. Similarly, the particles P_i may be interpolated between alternate nodes,

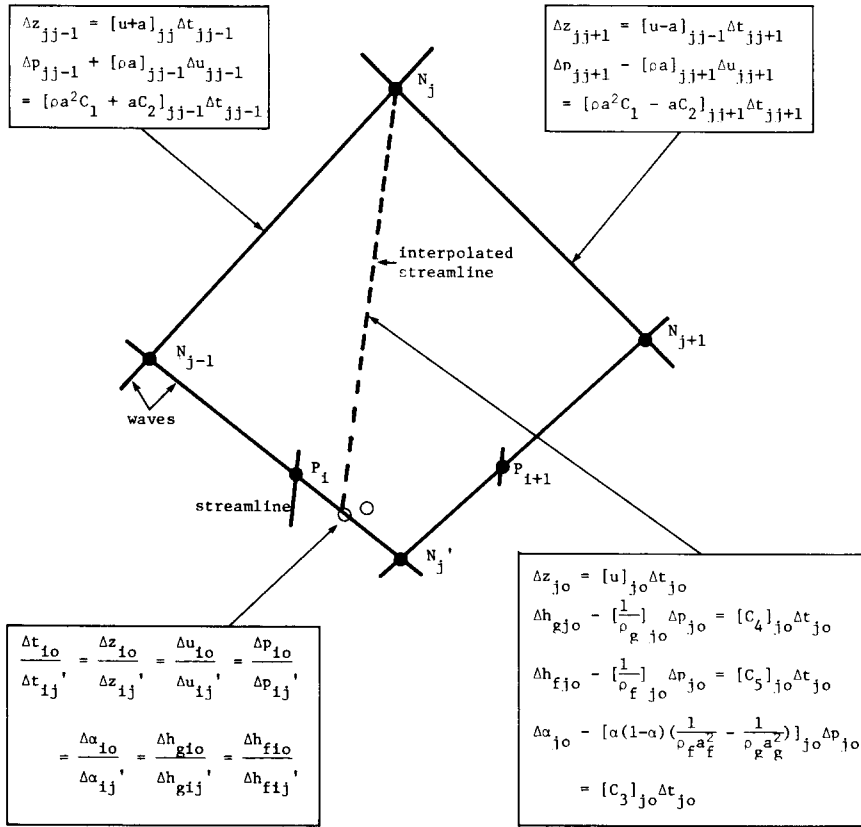


Figure 1. Algorithm used to advance a node from N_j to N_j ; P_i is a particle O the interpolated point; P_i and N_j are the nearest points to O on the line $N_{j-1}N_j$ in this example.

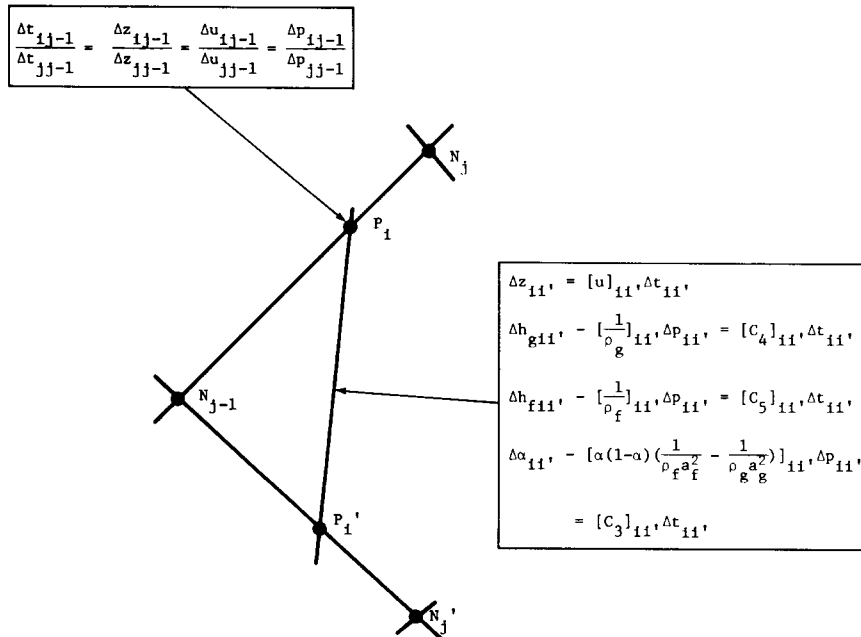


Figure 2. Algorithm used to advance a particle from P_i' to P_i .

N_{j-2} and N_j or N_j and N_{j+2} . The first scheme, in which the interpolations are always along characteristics, has been found to be preferable.

Boundaries must be treated specially. At an outflow boundary (see figure 3a), one of the characteristics lies outside the system. The two equations pertaining to this characteristic are replaced by $z = z^*$ and $p = p^*$, where z^* and p^* are given (p^* may be a function of time). At an inflow boundary (see figure 3b), we use $z = z^*$, $p = p^*$, $\alpha = \alpha^*$, $h_g = h_g^*$, $h_f = h_f^*$, together with the two equations for the one characteristic lying within the system. At a closed boundary (see figure 3c), $z = z^*$, $u = 0$, and the three streamline equations [18]–[20] plus the two equations for the characteristic internal to the system are used. In the event of supersonic flow at an open boundary, when the above algorithm gives $|u| > a$, the equation $p = p^*$ is replaced by $|u| = a$, and p is adjusted iteratively until this choking condition is satisfied.

The algorithm described here is a straightforward generalization to the EVUT model of one which has been previously used for the EVET model (Hancox *et al.* 1975). The advantage of such a scheme, in which characteristic paths are followed throughout, is its small numerical diffusion. Since discontinuities in the solution must propagate along characteristics, methods

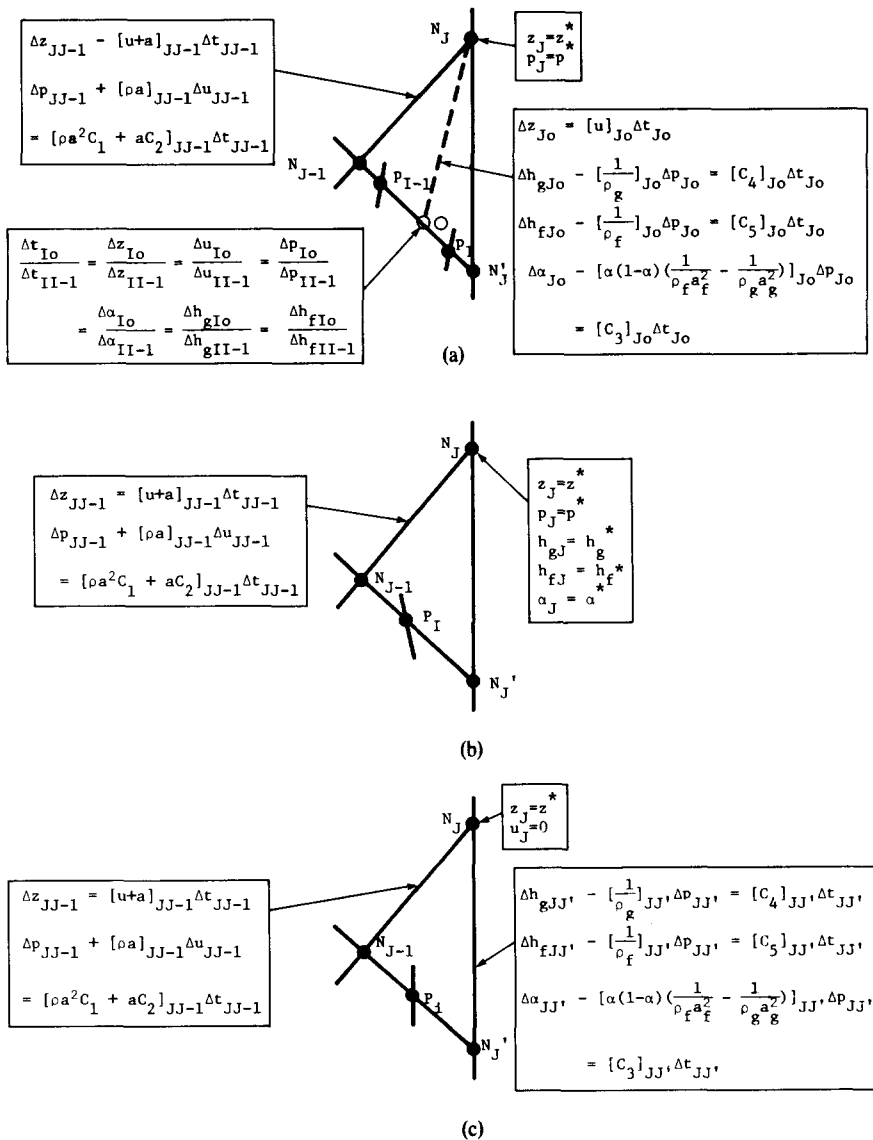


Figure 3. Algorithm used to advance a node at a boundary from N'_j to N_j : (a) Outflow boundary; (b) Inflow boundary; (c) Closed boundary.

which do not trace the characteristics will diffuse any discontinuities. This is true even for those method of characteristics solution schemes in which a fixed grid of points in space and time is used. On the other hand, if one wishes to study the flow at a given time or point in space, one must interpolate between the solution points given by the wave-tracing algorithm. This implies that some numerical diffusion will be present in plotted results, with scale length (or time) somewhat smaller than the mesh spacing (this is usually considerably smaller in these benchmark runs than it would normally be in a finite difference solution). However, and in contrast to finite difference schemes, this diffusion is not present in the actual solution, and its effects do not accumulate as the solution proceeds in time.

In practice, it is necessary to deviate somewhat from the algorithm outlined above. Since the sound speed is a very sensitive function of α , very rapid, but continuous changes may occur in the solution. In regions where such changes are present, it is necessary to use a very fine mesh. Since it is computationally inefficient to use such a fine mesh where it is not needed, a scheme for adding and deleting waves is necessary. By doing all interpolations along characteristics, we attempt to minimize spurious numerical effects introduced by this restructuring of the mesh.

This wave-tracing algorithm has been shown to have much less numerical diffusion than finite difference methods (Hancox *et al.* 1975). However it is much slower, and more difficult to program. In addition, because of the iterative technique required to obtain the solution at each point, it is extremely sensitive to irregularities in the fluid properties and source terms. If the fluid properties (ρ_k , $\partial\rho_k/\partial\rho$, $\partial\rho_k/\partial h_k$, η_k and h_{ks}) or externally specified quantities (dA/dz , dZ/dz , D_e , K/l and q_{wk}) are discontinuous, we can expect difficulties. The fluid properties are calculated by table lookup and linear interpolation, thus ensuring continuity. However, the extremely rapid changes in sound speed still cause problems.

STANDARD PROBLEMS

The algorithm outlined here has been tested on two standard problems, for which solutions have been obtained previously using the EVET model with both a method of characteristics and a finite difference algorithm (Hancox & Banerjee 1977). The first of these problems involves the transient created by application of a uniform heat source to a vertical upward flow of water in a pipe. The flow parameters are such that the equilibrium state, nearly reached after approx. 7 sec, is one in which the void fraction at the outlet is ~ 0.6 . Therefore a stationary boiling "front" is present. The second problem is based on the experiment of Edwards and O'Brien (1970) and involves the blowdown of a horizontal, closed-end pipe containing high enthalpy water, which is suddenly opened at one end to atmospheric pressure.

The initial conditions, boundary conditions, and externally specified parameters for the first problem are given in table 1. The friction factor was not that specified earlier; instead, the simpler model $f = 0.005$ was used to agree with the previous EVET predictions. The model used for q_{ik} , namely $q_{ik} = \alpha_f \alpha_g A \rho_k (h_{ks} - h_k) / t_{ik}$, as described previously, is of considerable interest. This formula is as simple as possible while satisfying the mathematical requirements of the model. The enthalpy difference was used instead of the temperature difference, mainly to avoid small discontinuity problems with the steam-water property routines at the saturation line, but as long as $\partial c_{pk} / \partial h_k$ is not large, the two will be nearly equivalent. The energy conservation equation contains terms of the following form:

$$\frac{\partial h_k}{\partial t} + \dots = \frac{(1 - \alpha_k)(h_{ks} - h_k)}{t_{ik}} + \dots$$

Neglecting the other terms for the moment, we note that a first-order explicit finite difference approximation to this equation will not give an adequate representation of the solution unless the time step $\Delta t < t_{ik}/(1 - \alpha_k)$; time steps $\Delta t > 2t_{ik}/(1 - \alpha_k)$ will in fact lead to numerical instability. With a finite difference algorithm, it is possible to reduce Δt to ensure that these

Table 1. Parameters for first standard problem

Initial conditions

$$u = 1.089 \text{ msec}$$

$$p = \begin{cases} 7.102 \text{ MPa, } z = 0.0 \text{ m} \\ 6.984 \text{ MPa, } z = 7.316 \text{ m} \\ \text{linearly interpolated, } 0.0 \text{ m} < z < 7.316 \text{ m} \end{cases}$$

$$\alpha = 0.0$$

$$h_f = 1.1847 \text{ MJ/kg}$$

$$h_g = h_{gs}$$

Boundary conditions

At $z = 0.0 \text{ m}$:

$$p = 7.102 \text{ MPa}$$

$$\alpha = 0.0$$

$$h_f = 1.1847 \text{ MJ/kg}$$

$$h_g = h_{gs}$$

At $z = 7.316 \text{ m}$:

$$p = 6.984 \text{ MPa}$$

Parameters

$$A = 127.0 \text{ mm}^2$$

$$dA/dz = 0.0 \text{ m}$$

$$dZ/dz = 1.0$$

$$f = 0.005$$

$$D_e = 4.33$$

$$K/l = \begin{cases} 0.0 \text{ m}^{-1}, 0.0 \text{ m} < z < 1.181 \text{ m} \\ 1.31 \text{ m}^{-1}, 1.181 \text{ m} < z < 2.690 \text{ m} \\ 1.52 \text{ m}^{-1}, 2.690 \text{ m} < z < 7.316 \text{ m} \end{cases}$$

$$q_w = \begin{cases} 9.0 \text{ kW/m}, 2.690 \text{ m} < z < 5.971 \text{ m} \\ 0.0 \text{ kW/m, elsewhere} \end{cases}$$

$$t_{if} = 0.01 \text{ sec}$$

$$t_{ig} = 0.01 \text{ sec}$$

conditions are satisfied, although in practice this may not be acceptable because of the resulting increase in computation time. With the wave-tracing algorithm, the only way to reduce Δt is to reduce the spatial separation of the waves, and this causes a large increase in computation time as well as an increase in storage requirements. Therefore, we are forced to choose t_{ik} sufficiently large to correspond with the computational mesh. In the first standard problem, approx. 80–100 waves in each direction were used. This led to the choice $t_{ik} = 0.01 \text{ sec}$, since smaller values produced difficulties during the transient and caused the solution procedure to fail.

In attempting to simulate physical problems, one should of course specify t_{ik} on physical grounds, and then adjust Δt as necessary to obtain stability. However, in our case we are using the program primarily to perform mathematical benchmark testing and to study the mathematical model. Therefore we are free to adjust parameters such as t_{ik} for reasons of convenience, although it is still desirable not to deviate from the real world by unnecessarily large amounts.

The mass flow rates, G , at the inlet and outlet, as predicted using the equilibrium (EVET) and non-equilibrium (EVUT) models, are plotted in figures 4 (inlet) and 5 (outlet). The slightly different rates observed before the onset of boiling near $t = 1 \text{ sec}$, and in the final state at $t = 7 \text{ sec}$, are due to slight changes in the property routines between the two runs. The delay in the onset of the transient in the EVUT model is related to the choice of t_{ik} ; smaller values of t_{ik} produced smaller delays, but it was not possible to follow these cases through the transient. This delay is made possible by storage of the applied energy in departures from equilibrium (i.e. superheating of the liquid), and the greater the delay, the larger the amount of energy stored in this form. Therefore, when boiling became significant, the effect on the flow was greater, and the transient was more severe, when larger values of t_{ik} were used. The EVET model

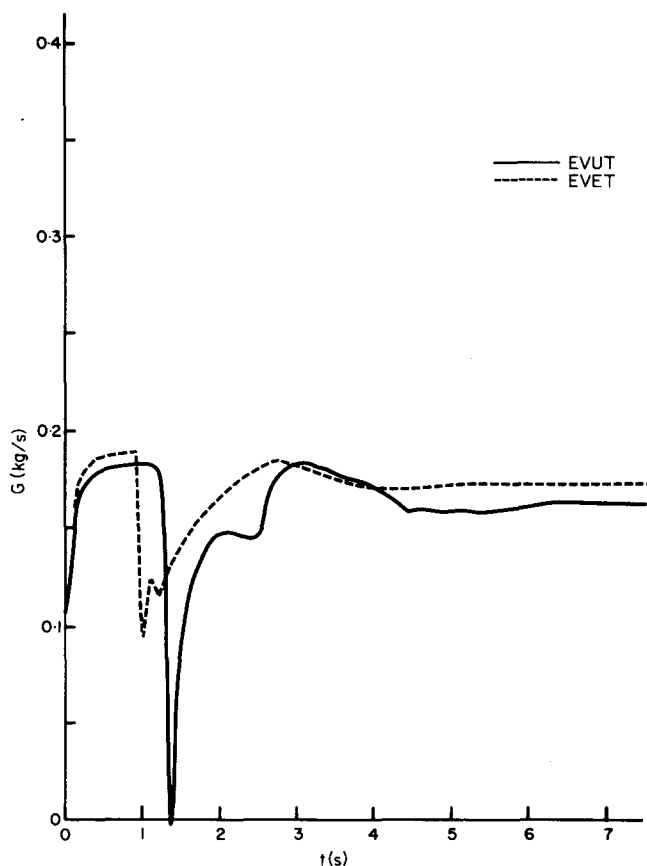


Figure 4. First standard problem—mass flow rate at inlet as predicted by EVET and EVUT wave-tracing programs.

corresponds to $t_{ik} = 0$. The subsequent behaviour of the mass flow rates was quite similar in the two models.

The pressure history at $z = 2.69$ m, using the EVUT model only, is given in figure 6. The natural period of pressure oscillations in this system, before boiling starts, is 0.014 sec, and only the envelope of these oscillations can be shown on this graph. Before the boiling transient, the pressure history consists of damped oscillations which were initiated by the application of the external heat source. These oscillations were also observed using the EVET model (the two models are identical for single-phase flow) but are not reproduced in finite difference solutions because of numerical diffusion. The pressure spike at the onset of boiling is both later and stronger than for EVET predictions. The subsequent pressure history is similar in the two models, but there is considerably more noise in the EVUT curve, on a short time scale. The source of this noise has not been investigated, but it may be due to interchange of energy between the two phases on the t_{ik} time scale, interacting with the natural pressure oscillations.

The flow quality history at the outlet is presented in figure 7 and the quality profile at $t = 7$ sec is presented in figure 8. The transition from single-phase to two-phase flow was successfully handled by a simple scheme for adding and deleting waves, based on the ratio of slopes of neighbouring waves. This simple scheme runs into difficulties when the transition is steeper, as shown by the second problem.

The second standard problem was a simulation of the Edwards & O'Brien (1970) blowdown experiment. The initial conditions, boundary conditions, and parameters are given in Table 2. It was not possible to drop the pressure instantaneously to atmospheric pressure at the outlet because of numerical difficulties. When an expansion fan was used to represent and instantaneous drop from 7.0 to 0.1 MPa at the outlet, the calculations became rapidly unstable. It

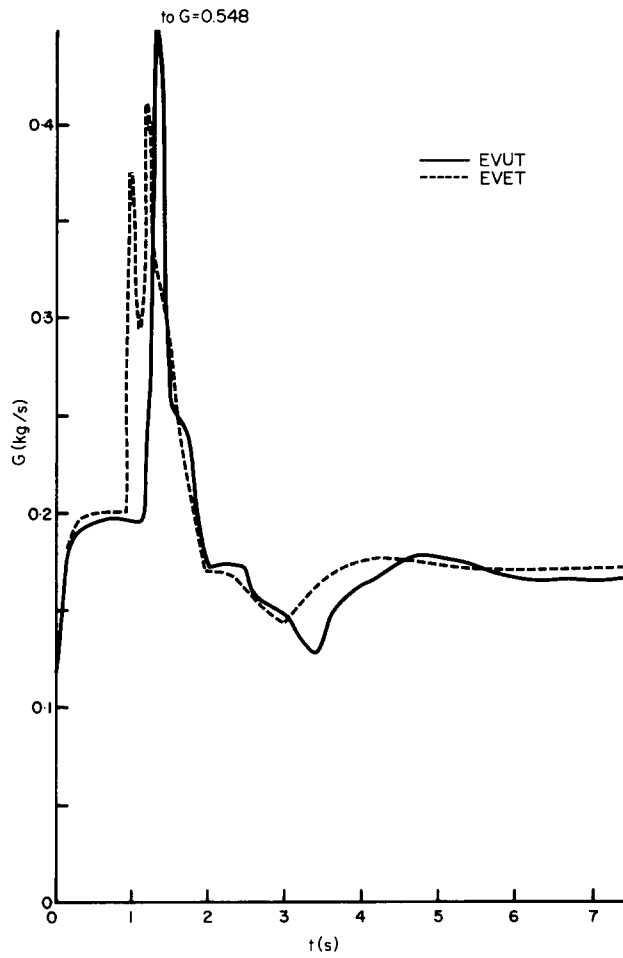


Figure 5. First standard problem—mass flow rate at outlet as predicted by EVET and EVUT programs.

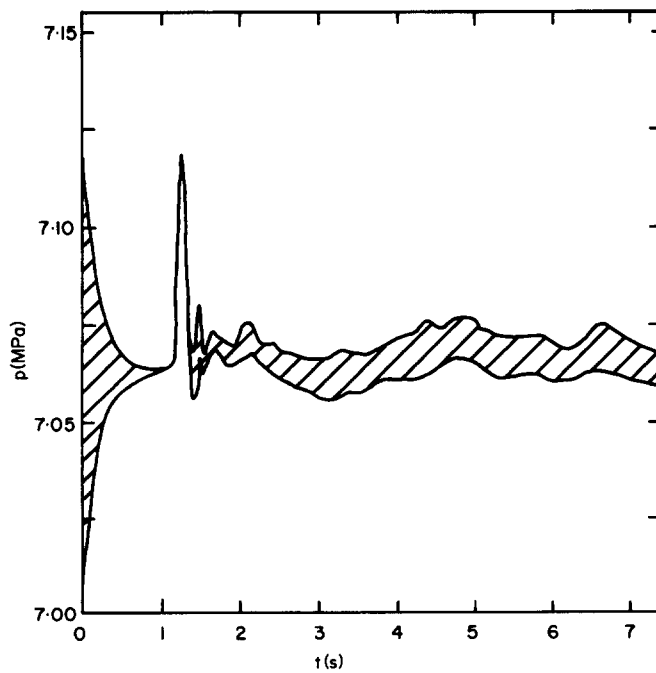


Figure 6. Approximate envelope of pressure history at $z = 2.69$ m in first standard problem (EVUT).

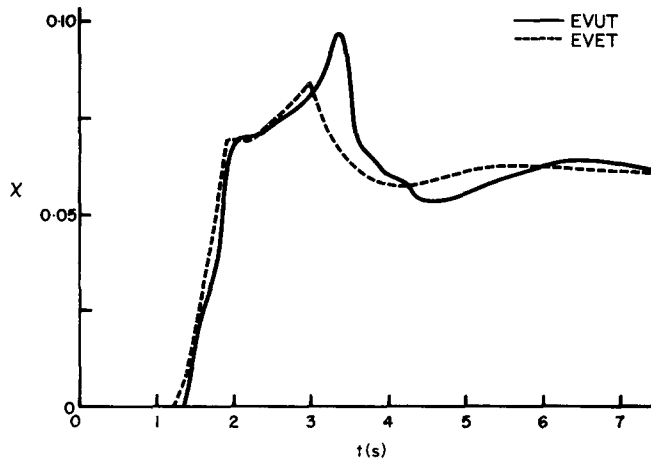


Figure 7. Flow quality at outlet in first standard problem as predicted by EVET and EVUT programs.

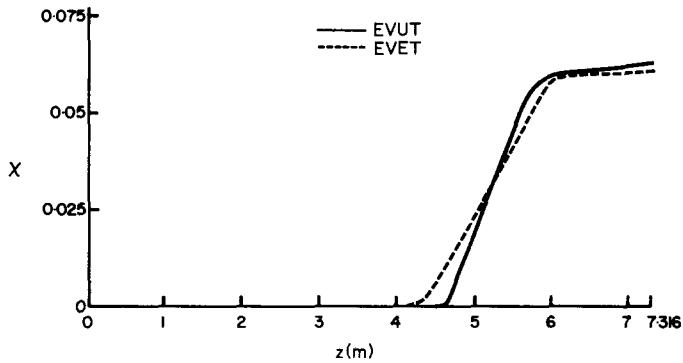


Figure 8. Flow quality at $t = 7.0$ sec in first standard problem as predicted by EVET and EVUT programs.

Table 2. Parameters for second standard problem

Initial conditions

- $u = 0.0$ m/sec
- $p = 7.0$ MPa
- $\alpha = 0.0$
- $h_f = 1.0459$ MJ/kg
- $h_g = h_{g_s}$.

Boundary conditions

At $z = 0.0$ m:

$$u = 0.0 \text{ m/sec}$$

At $z = 4.0$ m:

$$p = \begin{cases} 3.4 \text{ MPa, } t = 0.0 \text{ sec} \\ 0.1 \text{ MPa, } t > 0.005 \text{ sec} \\ \text{linearly interpolated, } 0.0 \text{ sec} < t < 0.005 \text{ sec.} \end{cases}$$

Parameters

- $A = 804.2$ mm²
- $dA/dz = 0.0$ m
- $dZ/dz = 0.0$
- $D_e = 32.0$ mm
- $K/l = 0.0$ m⁻¹
- $q_w = 0.0$ W/m
- $t_{if} = 0.005$ sec
- $t_{ig} = 0.005$ sec

was necessary to replace this fan by a two-point expansion fan from 7.0 to 3.4 MPa, just above saturation pressure, followed by a rapid, but not instantaneous, drop to 0.1 MPa. The time taken for this drop was set at 5 msec, since shorter times gave difficulty. The pressure drop at the closed end appeared to be instantaneous, within the resolution of the mesh used (see figure 9). This indicates that the effects of this slower drop were probably not serious.

In previous simulations, using the EVET model, a striking difference between the computed and experimental results is the undershoot in pressure at the closed end seen in the experiment, but not present in the EVET simulation. In the experiment, when the pressure wave reached the closed end, the pressure dropped to approx. 1.5 MPa, and then rose to near 3 MPa within a few milliseconds. This undershoot is attributed to departures from local thermal equilibrium, and this is borne out by the EVUT results. These show a sudden drop in pressure followed by a slower increase. The lowest pressure reached, and the rate of increase, depend on the heat transfer times t_{ik} (see figure 9); unfortunately, numerical difficulties prevented the use of times small enough to match the experimental curve. These difficulties, as noted before, are related not to the specific heat transfer model used, but rather to the time scale of the transfer process. Similar problems have been encountered in tests using an implicit finite difference code based on the characteristic finite difference procedure (Mathers *et al.* 1976).

In addition to the case with $t_{if} = t_{ig} = 5$ msec, a number of other cases were tried. Halving t_{ik} gave a closer fit to the experimental curve, but this run failed near $t = 40$ msec, well before the maximum in the pressure at the closed end had been reached, and a smaller t_{ik} caused earlier failure. Larger values of t_{ik} ran successfully, resulting in a deeper pressure minimum and a slower rise. Cases in which $t_{if} \neq t_{ig}$ failed whenever the smaller of the two became less than a few milliseconds. More complicated models for q_{ik} , in which t_{ik} became smaller with increasing $|T_s - T_k|$, also failed under the same conditions.

The relatively slow heat transfer has other effects besides those noted in the behaviour of the pressure at the closed end. In particular, the temperatures of the two phases are found to be

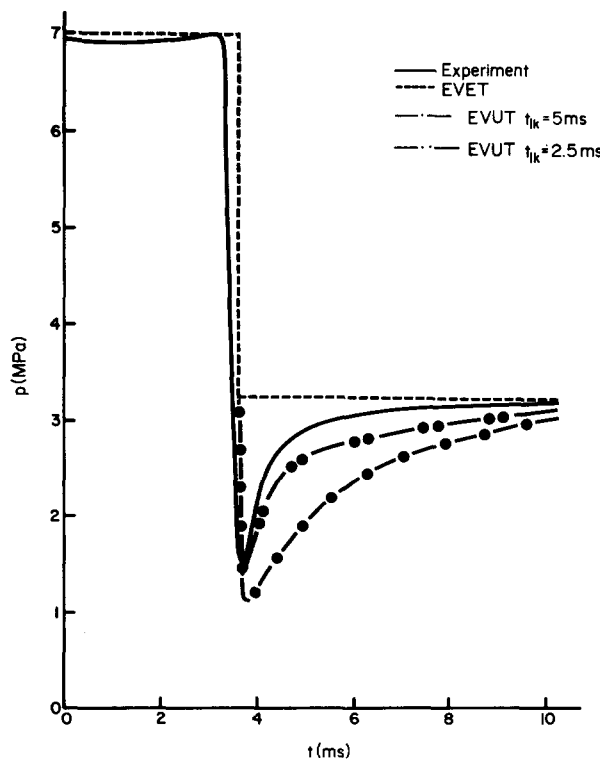


Figure 9. Pressure at closed end in second standard problem—experimental, EVET and EVUT ($t_{ik} = 5$ and 2.5 msec) results.

far from the saturation value, even when the void fraction is substantial. For example, at $t = 0.005$ sec, the liquid, saturation and vapour temperatures at the closed end were 236, 153 and 27°C respectively, and $\alpha = 0.72$. At $t = 0.072$ sec, when the pressure at the closed end was maximum, these three temperatures were 218, 188 and 115°C, with $\alpha = 0.87$. The large deviations are due to the fact that adiabatic expansion of the vapour dominates the interfacial heat transfer. Larger values of t_{ik} led to even greater discrepancies.

While one might expect the liquid temperature to stay near its original value, the deviations from equilibrium for the vapour phase seem unreasonably large. During the late stages of the blowdown, it was possible to decrease t_{ig} by a factor of 100 and thereby accelerate the approach of T_g to T_s . However, as noted earlier, it was not possible to use such a small value of t_{ig} during the earlier part of the run. This suggests that the use of a constant t_{ig} may be unrealistic, and that more sophisticated relationships might be desirable.

Another model, in which the enthalpy equation for the vapour is replaced by $h_g = h_{gs}(p)$, has been constructed. Note that in this model, the vapour sound speed differs from that in the EVUT model, since the vapour is constrained to stay at the saturation line; $a_g^{-2} = (\partial\rho_g/\partial p) + (\partial\rho_g/\partial h_g)(dh_{gs}/dp)$ in this model. This results in a vapour sound speed which is 10–20% lower than in the EVUT model. In the calculations for the second standard problem, the two models gave very similar results, except of course for the vapour temperature. This indicates that despite the large temperature drop in the vapour in the EVUT model, relatively little energy is involved, since its effect on the flow is small. The major effects of the departure from thermal equilibrium are those related to the liquid.

In figure 10 the void fraction α , at a position 1.4 m from the closed end, is plotted as a function of time. The curve for the alternative model, in which $h_g = h_{gs}$, is virtually identical with that for the EVUT model. It appears that the major part of the discrepancy between the simulations and the experiment may be due to phase separation effects (i.e. different velocities for liquid and vapour), since the EVET and EVUT results are quite similar.

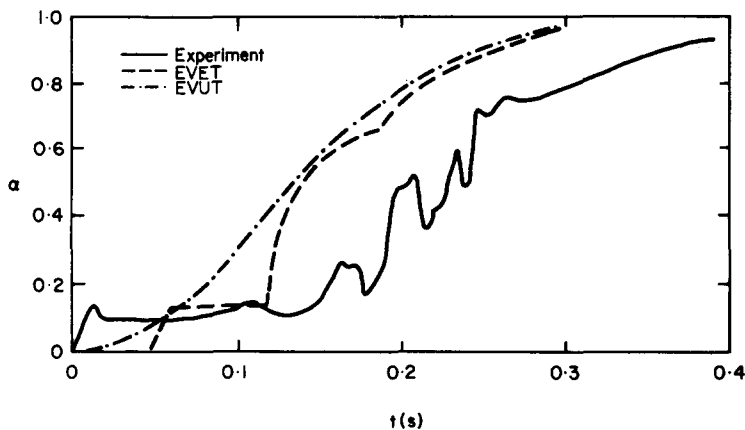


Figure 10. Void fraction α , 1.4 m from closed end, in second standard problem-experimental, EVET and EVUT results.

DISCUSSION

In addition to its uses for benchmark testing of faster codes, the wave-tracing method has considerable usefulness in studying effects related to the choice of mathematical model, because of its freedom from most spurious numerical effects. Once such numerical effect which is still present is the limitation on t_{ik} imposed by the finite value of Δt . We might try to overcome this limitation in a number of ways. One way is to perform calculations with larger values of t_{ik} and then extrapolate the results to smaller values. This is of questionable accuracy in cases where the flow variables themselves change greatly on a short time scale, as in the

second standard problem. Another is to use very small time steps to allow small t_{ik} , but this is too inefficient for most practical situations. A third way is to use higher-order finite difference approximations to the derivatives, again with associated computational costs. Yet another is to effect a change of variables in such a way that the offending term is formally removed from the enthalpy equation. This is similar in effect to using a derivative model for q_{ik} , and has the undesirable effect of making the structure of the equations dependent on the model chosen for q_{ik} . It is not at all clear at present which, if any, of these attempts would be most acceptable. It should also be noted that we are trying to represent interphase heat transfer during transients, where experimental data relevant to choices for parameters, and functional forms, are missing.

At any rate, further studies of various formulations for q_{ik} are desirable. In particular, the assumption that $A_i \propto \alpha_f \alpha_g A$ used in the present calculations is undoubtedly a poor representation of the physical reality, and more advanced formulae are desirable. Indeed, a slightly more complicated model was used in practice; at the transition from single-phase to two-phase flow, this assumption implies $q_{if} = q_{ig} = m_{ig} = 0$. In order to achieve non-zero α_k , we set $\alpha_k = \epsilon$ ($\epsilon \sim 10^{-6}$) at the onset of local boiling or condensation. (This is effectively similar to assuming the existence of a finite level of nucleation sites.) The wave-tracing method seems well-adapted to studying the effects of various such formulae, because of its relative lack of numerical diffusion effects.

One numerical problem with this method which is not present in finite difference codes is the difficulty in handling rapid transitions from single-phase to two-phase flow, caused by the large changes in sound-speed between neighbouring mesh points. These transitions are automatically broadened by numerical diffusion, and one way of eliminating the difficulty might be to introduce some artificial diffusion. This approach is somewhat similar to that of pseudo-viscosity techniques (Richtmyer & Morton 1967). Another way would be to replace the rapid transition by an artificial discontinuity, treated like a boiling boundary in the EVET model (Hancox & Banerjee 1977).

The EVUT model has potential applications in situations where rapid changes in α occur, as in the second standard problem, and in situations where external heat input prevents the flow from reaching local thermal equilibrium, as in the first standard problem (see figure 8). Since the major effects of non-equilibrium are due to superheating or subcooling of the liquid phase, the model in which the vapour is tied to the saturation line (when $\alpha < 1$) may be adequate. In cases where a significant part of the heat flow is carried by the vapour phase, it is likely that different velocities in the two phases will be present. In such cases (e.g. stratified or annular flow), a model in which the velocities and pressures of the two phases are different (UVUTUP) may be necessary.

The EVUT model also has applications during the development of more advanced unequal-velocity models. The interfacial heat and mass transfer terms in this model will also appear in more sophisticated models (such as UVUTUP models). The EVUT model supplies a convenient medium for studying these terms independently of the added complications due to unequal velocities and/or pressures. Indeed, it may prove possible to use an accurate solution scheme like this one to throw more light on interfacial exchanges, in conjunction with experiments in which the assumptions of equal velocities and pressures are satisfied.

It is interesting to note that, despite the simple formula used for the heat transfer terms q_{ik} , the EVUT model appears to be capable of calculating the early behaviour of the transient in the second problem reasonably well. This suggests that the precise form chosen for q_{ik} may not be a critical factor in performing simulations of more complicated experiments with faster finite-difference codes.

SUMMARY

A wave-tracing, or method of characteristics, algorithm has been implemented for the EVUT model of one-dimensional two-phase flow. This method has been checked on two

standard problems. Agreement with previous calculations, using the EVET model, and using a finite difference algorithm for the EVUT model, is satisfactory. This algorithm has greatly reduced numerical diffusion effects as compared with finite difference schemes. Therefore, despite its slowness, it is useful for benchmark testing of these codes, and for studying various models of the interfacial heat transfer process, and it is now being used for these purposes.

Acknowledgements—The author wishes to thank Dr. W. T. Hancox, Mr. D. Kawa, Dr. W. G. Mathers and Dr. B. H. McDonald for their advice and assistance during the development of this code.

REFERENCES

- BANERJEE, S., FERCH, R. L., MATHERS, W. G. & McDONALD, B. H. 1978 The dynamics of two-phase flow in a duct. *6th Int. Heat Transfer Conf.*, Toronto.
- BOURE, J. A. 1973 Dynamique des écoulements diphasiques: Propagation des petites perturbations. Centre d'Etudes Nucleaires de Grenoble Rep. CEA-R-4456.
- BOURE, J. A., BERGLES, A. E. & TONG, L. S. 1973 Review of two-phase flow instability. *Nucl. Engng Design* **25**, 165–192.
- BRITTIAN, I. & FAYERS, F. J. 1976 A review of UK developments in thermalhydraulic methods for loss of coolant accidents. *Proc. CSNI Specialists Meeting on Transient Two-Phase Flow*, Toronto. (Edited by WEAVER K. R. & BANERJEE S.), AECL, Mississauga, Ontario, May 1978.
- EDWARDS, A. R. & O'BRIEN, T. P. 1970 Studies of phenomena connected with the depressurization of water reactors. *J. Br. Nucl. Energy Soc.* **9**, 125–135.
- HANCOX, W. T. & BANERJEE, S. 1977 Numerical standards for flow-boiling analysis. *Nucl. Sci. Engng* **64**, 106–123.
- HANCOX, W. T., MATHERS, W. G., & KAWA, D. 1975 Analysis of transient flow-boiling: Application of the method of characteristics. Paper 42, *AICHE-ASME 15th National Heat Transfer Conf.*, San Francisco.
- HANCOX, W. T. & NICOLL, W. B. 1972 A wall shear stress formula for adiabatic two-phase flow. Unpublished Westinghouse Canada Limited report.
- MARTINI, R., PIERINI, G. C. & SANDRI, C. 1976 A one-dimensional transient two-phase flow model and its implicit finite different solution. *Proc. CSNI Specialists Meeting on Transient Two-Phase Flow*, Toronto. (Edited by WEAVER K. R. & BANERJEE S.), AECL, Mississauga, Ontario, May 1978.
- MATHERS, W. G., ZUZAK, W. W., McDONALD, B. H. & HANCOX, W. T. 1976 On finite difference solutions to the transient flow-boiling equations. *Proc. CSNI Specialists Meeting on Transient Two-Phase Flow*, Toronto. (Edited by WEAVER K. R. & BANERJEE S.), AECL, Mississauga, Ontario, May 1978.
- RIGHTMYER, R. D. & MORTON, K. W. 1967 *Difference Methods for Initial-Value Problems*. Interscience, New York.
- SOLBRIG, C. W., MORTENSEN, G. A. & LYCZKOWSKI, R. W. 1976 An unequal phase velocity, unequal phase temperature theory applied to the two-phase blow-down from a horizontal pipe. *Proc. 1976 Heat Transfer and Fluid Mechanics Institute*, Davis, p. 60. Standard Univ. Press, California.
- TURNER, W. J. & TRIMBLE, G. D. 1976 Calculation of transient two-phase flow. *Proc. CSNI Specialists Meeting on Transient Two-Phase Flow*, Toronto. (Edited by WEAVER K. R. & BANERJEE S.), AECL, Mississauga, Ontario, May 1978.